Available online at www.sciencedirect.com
SCIENCE DIRECT
Biochemical and Biophysical Research Communications 338 (2005) 762–770
BBRC
www.elsevier.com/locate/ybbrc

Co-culture of osteoblasts and chondrocytes modulates cellular differentiation in vitro

Jie Jiang [a], Steven B. Nicoll [b], Helen H. Lu [a,*]

[a] *Biomaterials and Interface Tissue Engineering Laboratory, Department of Biomedical Engineering, Columbia University, New York, NY 10027, USA*
[b] *Department of Bioengineering, University of Pennsylvania, Philadelphia, PA 19104, USA*

Received 30 September 2005
Available online 17 October 2005

Abstract

Biological integration of cartilage grafts with subchondral bone remains a significant clinical challenge. We hypothesize that interaction between osteoblasts and chondrocytes is important in regenerating the osteochondral interface on tissue-engineered osteochondral grafts. We describe here a sequential co-culturing model which permits cell–cell contact and paracrine interaction between osteoblast and chondrocytes in 3-D culture. This model was used to determine the effects of co-culture on the phenotypic maintenance of osteoblasts and chondrocytes. It was found that while chondrocytes synthesized a type II collagen and glycosaminoglycan (GAG) matrix, GAG deposition was significantly lower in co-culture. Alkaline phosphatase activity was maintained in osteoblasts, but cell-mediated mineralization in co-culture was markedly lower compared to osteoblast controls. These results collectively suggest that interactions between osteoblasts and chondrocytes modulate cell phenotypes, and the importance of these interactions on osteochondral interface regeneration will be explored in future studies.

Keywords: Co-culture; Osteoblasts; Chondrocytes; Osteochondral; Micromass

Osteoarthritis is the most common form of arthritis, with over 20 million Americans suffering from this degenerative condition [1]. During routine physical activities, articular cartilage breaks down and its continued wear exposes the subchondral bone to the synovial environment. If left untreated, the sustained physiological loading results in symptomatic pain, swelling, and eventually the loss of joint motion. Due to the limited regenerative capacity of adult articular cartilage, surgical intervention is required to treat osteoarthritis [2].

Existing treatment options for the repair of focal lesions and damage to the articular surface have had limited success [2]. Traditional methods such as debridement, subchondral bone drilling, and microfracture typically result in fibrocartilage formation at the defect site [2]. Other methods, such as autologous cell or tissue transfer via periosteal grafts and tissue adhesives, have poor long-term outcomes and are associated with severe side effects [3]. Autologous chondrocyte implantation involves the isolation and expansion of chondrocytes in culture and injection of these cells under a periosteal flap at the defect site [3]. Wider application of this procedure is restricted by the lack of inter-patient consistency, as evidenced by a recent long-term in vivo animal study which revealed little difference from the control group [4]. None of the existing cartilage grafting methods have been able to demonstrate stable integration either with the surrounding cartilage tissue or with the subchondral bone. Thus, the regeneration of the native osteochondral interface remains a significant clinical challenge.

Additional treatments for cartilage focal lesions with promising initial results are autologous osteochondral grafting procedures such as Mosaicplasty and Osteochondral Autograft Transfer System. In these procedures, osteochondral columns from a non-load bearing region

* Corresponding author. Fax: +1 212 854 8725.
E-mail address: hl2052@columbia.edu (H.H. Lu).

0006-291X/$ - see front matter © 2005 Elsevier Inc. All rights reserved.
doi:10.1016/j.bbrc.2005.10.025

are surgically removed and transplanted into the defect site. While these grafts have shown good clinical results, they are limited by supply and donor site morbidity [2]. The ideal graft for the treatment of articular cartilage defects should be mechanically functional and able to structurally and functionally integrate with the host tissue [5]. Due to limitations with current treatment options for cartilage defects, there is a sustained interest in tissue-engineered solutions for cartilage repair and regeneration [6–15]. Several groups have reported on the development of tissue-engineered osteochondral grafts, which may have application in a clinical setting [16–23]. The long-term success of such grafts will depend largely on their ability to integrate with host tissue and to regenerate the osteochondral interface.

Currently, it is not well understood how the interface between bone and cartilage can be regenerated during cartilage repair. We hypothesize that the interaction between osteoblasts and chondrocytes is important in initiating the events which lead to interface regeneration. The potential of osteoblasts to regulate chondrocyte metabolism was first reported by Lacombe-Gleize et al. using a monolayer, trans-well insert co-culture model. It was found that osteoblasts up-regulated the mitotic potential of chondrocytes through TGF-β1 secretion [24]. Further interpretation of these results was limited by the fact that chondrocytes in this study were grown in monolayer instead of 3-D culture. A significant challenge in osteoblast–chondrocyte co-culture is that, unlike osteoblasts which are anchorage-dependent, chondrocytes de-differentiate and lose their phenotype in monolayer cultures [25].

Therefore, to test our hypothesis that chondrocytes and osteoblasts will modulate each other's phenotypic responses under physiological conditions, we have designed a simple and reliable 3-D co-culture model to study the interaction between osteoblasts and chondrocytes. In this co-culture model (Fig. 1), a sequential culturing protocol is used whereby chondrocytes are initially seeded in high density micromass cultures, after which osteoblasts are introduced and allowed to directly adhere to the chondrocyte micromasses. This novel co-culture model also mimics the initial point of contact between a tissue-engineered cartilage construct populated with chondrocytes and the subchondral bone upon implantation. The objectives of this study were (1) to validate the co-culture model; (2) to evaluate the effects of co-culture on the growth and phenotypic maintenance of osteoblasts and chondrocytes. It is anticipated that osteoblasts and chondrocytes can be co-cultured together in direct physical contact while maintaining their respective phenotype. Results of this study will support the efforts to elucidate the mechanism of regenerating the osteochondral interface on tissue-engineered grafts.

Materials and methods

Cells and cell culture. Primary bovine articular chondrocytes and osteoblasts were utilized in this study. Bovine articular chondrocytes were isolated from full-thickness articular cartilage of carpometacarpal joints of 2- to 6-month-old calves from a local abattoir (Green Village, NJ). Articular cartilage tissue was excised from the exposed carpometacarpal joint surface and minced into small pieces. Chondrocytes were obtained following serial enzymatic digestions of the cartilage tissue by modifying the method described by Mauck et al. [11]. The tissue was first digested for 1 h in a 0.25% protease (Calbiochem, San Diego, CA) solution dissolved in Dulbecco's modified Eagle's medium (DMEM, Cellgro-Mediatech, Herndon, VA), followed by 4 h of 0.05% collagenase (Sigma, St. Louis, MO) digestion. The isolated chondrocytes were maintained in fully supplemented medium, which consisted of DMEM with 10% fetal bovine serum (FBS, Cellgro-Mediatech), 1% non-essential amino acids, and antibiotics (100 U/mL penicillin, 100 mg/mL streptomycin, Cellgro-Mediatech).

Primary bovine osteoblast cultures were established from explant cultures of long bone fragments taken from the same joint used for

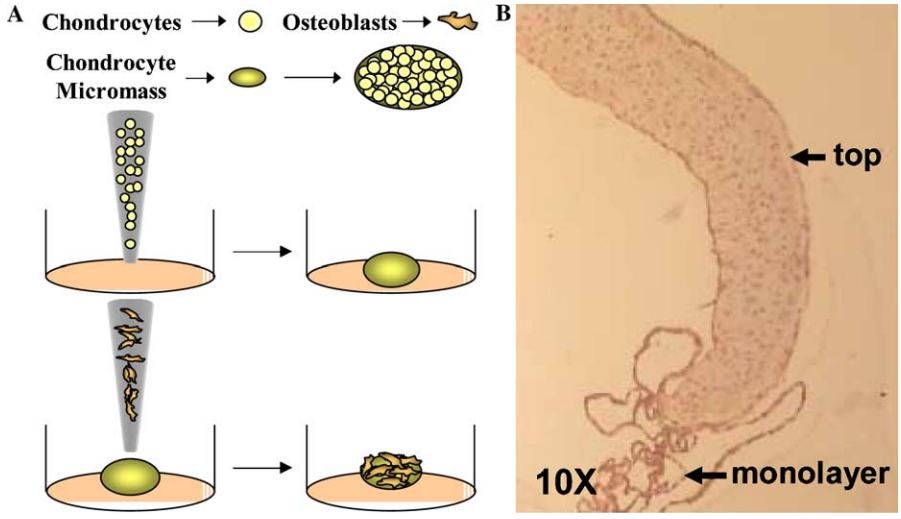

Fig. 1. (A) Schematic of the co-culture model of osteoblasts and chondrocytes. The chondrocyte micromass is first formed by plating a high density chondrocyte suspension (2×10^7 cells/mL) on pre-sterilized coverglass. The chondrocytes were allowed to adhere for 1 h, after which a drop of bovine osteoblast suspension (5×10^6 cells/mL) was added to the chondrocyte micromass. The osteoblasts were then allowed to adhere on the micromass for an another hour prior to the addition of media. (B) Cross-sectional H&E staining to visualize cell distribution.

chondrocyte isolation, following the methods of Spalazzi et al. [26]. Briefly, the bone fragments were excised from the tibia of the same calves using a bone cutter. The fragments were washed twice with phosphate-buffered saline (PBS) and cultured in supplemented DMEM. Cell outgrowth was generally observed after 1 week of culture and only cells from the second migration were used for the study, as they are reported to be more osteoblast-like and homogeneous in culture [27]. All cell cultures were maintained under humidified conditions at 37 °C and 5% CO_2.

Osteoblast–chondrocyte co-culture model. The primary osteoblast–chondrocyte co-culture model developed in this study is based on the combined culture of a high density chondrocyte micromass and a monolayer of osteoblasts. As shown in Fig. 1A, a high density micromass of chondrocytes was first formed, followed by adhesion of osteoblasts on top of the micromass. Chondrocyte micromasses were established following the methods of Ahrens et al. [28]. Specifically, chondrocytes were trypsinized and re-suspended in the culturing media at a concentration of 2×10^7 cells/mL. For each individual micromass, chondrocytes (10 μL) were first plated on pre-sterilized coverglass (VWR, West Chester, PA) and then incubated for 1 h. Subsequently, bovine osteoblasts (10 μL at 5×10^6 cells/mL) were seeded directly on top of the chondrocyte micromass. The osteoblasts were allowed to adhere onto the chondrocyte micromass for an additional hour, after which supplemented DMEM with 50 μg/mL L-ascorbate (Sigma) was added to the culture.

To better emulate the physiological environment, an alternate model which reverses the order of cell seeding was also examined in this study. In this second co-culture model, the chondrocyte micromass was formed atop a pre-existing osteoblastic monolayer. The osteoblasts and chondrocytes were plated at the same density as in the first model. For both co-culture models, chondrocyte micromasses alone and osteoblast monolayers seeded in tissue culture plates at a density of 1.5×10^4 cells/cm^2 served as controls.

In order to validate the co-culture model and to determine the respective location of each cell type, osteoblasts were pre-labeled with the CM-DiI cell tracking dye (Molecular Probes, Eugene, OR) using manufacturer's recommended protocol. Cell distribution was imaged at specific time points using fluorescence microscopy after nuclear counterstain with 4′,6-diamidino-2-phenylindole (DAPI, Sigma). All samples were grown in supplemented DMEM with 50 μg/mL of ascorbic acid (Sigma). For mineralization, 3.0 mM of β-glycerophosphate (β-GP, Sigma) was added to the co-culture experimental group, chondrocyte micromass, and osteoblast monolayer control on day 7. The samples were harvested at 1, 3, 7, 14, and 21 days.

Cell proliferation–DNA quantification. Cell proliferation ($n = 5$) was determined by measuring total DNA per sample using the PicoGreen dsDNA assay (Molecular Probes) following the manufacturer's suggested protocol. Briefly, at the designated time points, the cells were lysed with distilled water and then homogenized. Fluorescence of the samples was measured with a microplate reader with excitation and emission wavelengths of 485 and 535 nm, respectively. The total number of cells in the sample was determined by converting the amount of DNA per sample to cell number using the conversion factor of 7.7 pg DNA/cell reported for bovine chondrocytes [29].

Gene expression. Gene expression was measured using the reverse-transcription polymerase chain reaction (RT-PCR, primers listed in Table 1). Total RNA was isolated using the Trizol (Invitrogen, Carlsbad, CA) extraction method. The isolated RNA was reverse-transcribed into cDNA using the SuperScript First-Strand Synthesis System (Invitrogen), and the cDNA product was amplified using recombinant Taq DNA polymerase (Invitrogen). All genes were amplified for 40 cycles in a thermal cycler (Eppendorf Mastercycler gradient, Brinkmann, Westbury, NY).

Sulfated glycosaminoglycan deposition. Glycosaminoglycan (GAG) content ($n = 5$) was quantified using the Blyscan 1,9-dimethylmethylene blue (DMMB) assay kit (Accurate Chemical, Westbury, NY) following the manufacturer's suggested protocol. Specifically, the samples were digested overnight at 60 °C in 2% Papain (Sigma). After digestion, 100 μL of the digest was added to 1 mL of the Blyscan assay dye agent and mixed for an hour. The mixture was then centrifuged for 20 min at 10,000*g*. After removing the supernatant, the precipitate was re-suspended in 1 mL of Blyscan dissociation solution and the absorbance was measured at 620 nm using a microplate reader.

Alkaline phosphatase activity. Sample alkaline phosphatase (ALP) activity was determined using an enzymatic assay based on the hydrolysis *p*-nitrophenol phosphate (pNP-PO_4) to pNP [30]. Briefly, at the designated time points, cells were first lysed with Millipore filtered distilled water and then homogenized. Aliquots of the sample homogenate (25 μL) were added to 75 μL of 10 mM pNP-PO_4, and the solution was then incubated at 37 °C for 30 min. The reaction was terminated by addition of 100 μL of 0.1 N NaOH, and absorbance was measured at 410 nm using a microplate reader.

Extracellular matrix composition and distribution. Matrix composition and distribution were assessed using histological and immunohistochemical methods. For histological analysis, the samples were rinsed twice with PBS and then fixed in neutral formalin (Fisher Scientific, Tustin, CA). For paraffin-embedded samples, 7 μm cross-sections were sectioned and mounted prior to staining. For cellular distribution, all samples were stained with hematoxylin and eosin (H&E). GAG distribution was determined using Alcian blue staining [31]. Mineralization was ascertained using Alizarin red S staining [32]. Qualitative ALP activity was visualized on whole mount samples using an ALP cytochemistry kit (85L-2, Sigma) following manufacturer's suggested protocol.

For immunohistochemistry, samples were rinsed with PBS, fixed in acid formalin, and then embedded in paraffin. The paraffin blocks were sectioned as above. For collagen staining, samples were rehydrated and rinsed with PBS, and treated with 0.5 mg/mL hyaluronidase (Sigma) for 30 min to digest the GAG matrix and expose the collagen epitopes. The samples were swelled in 0.5 N acetic acid (Fisher Scientific) for 2 h at 4 °C. The samples were then blocked with 10% goat serum (Sigma) for 30 min and incubated at 4 °C overnight with primary antibodies to types I collagen (MAB3391, Chemicon, Temecula, CA) and type II collagen (II-II6B3, Developmental Studies Hybridoma Bank, Iowa City, AI). After rinsing with PBS, the samples were then stained with Alexa fluor-488 conjugated secondary antibodies (Molecular Probe) for 1 h at room temperature. Nuclear counterstaining with propidium iodide (Molecular Probes) was used to visualize the location of cells with respect to the matrix. The samples were imaged using confocal microscopy (Olympus IX70, Melville, NY) with dual excitation wavelengths at 488 and 568 nm.

Statistical analysis. Data are presented as means ± standard deviation. For statistical analysis, a two-way analysis of variance was performed to determine the effect of culture condition and time on cell number, GAG content, and ALP activity. A Tukey–Kramer post hoc test was used for all pairwise comparisons and statistical significance was set at $p < 0.05$. All statistical analyses were performed using the JMP statistical software package (SAS Institute, Cavy, NC).

Table 1
List of oligonucleotide primers used

Gene	Sense	Antisense	Size
GAPDH	GGTGATGCTGGTGCTGAGTA	ATCCACAGTCTTCTGGGTGG	305
Aggrecan	CACTGTTACCGCCACTTCCC	GACATCGTTCCACTCGCCCT	303
ALP	CTTCAGACTCTCAACACCAA	CCTCGATGTCCTTAATGTTG	524
Type I collagen	TGCTGGCCAACCATGCCTCT	TTGCACAATGCTCTGATC	489
Type II collagen	ATGACAACCTGGCTCCCAAC	GCCCTATGTCCACACCGA	359
Type X collagen	TCCAAAATACAGGTCTGAGC	CCTGTTAATTGTCAGAACAG	247

Results

Osteoblast–chondrocyte co-culture model

As shown in Fig. 1A, the osteoblast–chondrocyte co-culture model developed in this study combines 3-D culture of chondrocytes with an osteoblast monolayer. Fig. 1B shows H&E staining of a cross-section of the co-cultured system in which osteoblasts were seeded on top of the chondrocyte micromass. The order of cell seeding during co-culture had no measurable effect on the overall cellular response evaluated in this study. A monolayer of elongated cells was observed on the top layer of the micromass, while chondrocytes within the micromass maintained a spherical morphology. The entire micromass was comprised of about five to ten cell layers, and cells on the bottom of the micromass also assumed an elongated morphology. To definitively identify the location of osteoblasts with respect to chondrocytes, cell tracking confirmed that osteoblasts were found only atop the micromass and they were localized in the monolayer region after 1 week of culture (Fig. 2).

Cell proliferation

Total cell number within the micromass remained relatively constant over time for both the chondrocyte micromass control and the co-cultured samples (Fig. 3) [33].

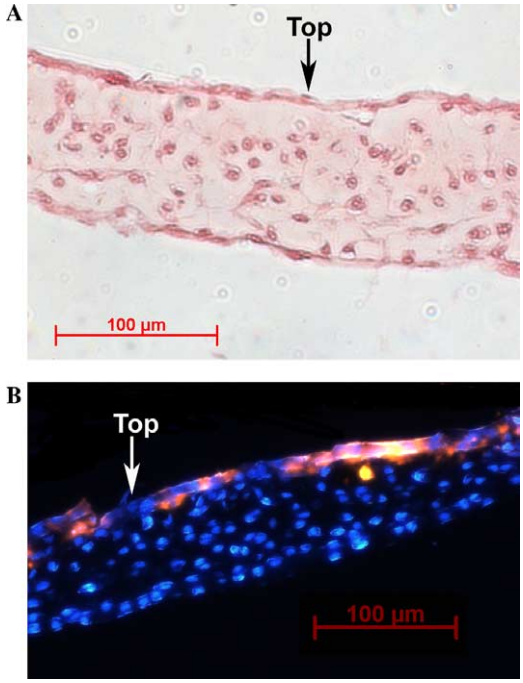

Fig. 2. Cross-section of co-cultured micromass. (A) H&E staining for visualization of cellular distribution within the micromass. Cells within the micromass exhibited a spherical morphology while cells at both the surface and surrounding monolayer were elongated (day 11). (B) Osteoblasts were tracked with CM-DiI dye (orange), and nuclei were stained with DAPI (blue). Osteoblasts were only seen as a thin layer on top of the micromass (day 7). (For interpretation of the references to color in this figure legend, the reader is referred to the web version of this paper.)

No statistical difference was observed between the control and co-culture group. The osteoblast monolayer control group proliferated over the 3-week culture period, and cells reached confluence by day 7. Cells at the edge of the micromass proliferated and migrated from the culture over time. An observable monolayer surrounded the micromass at day 3, and a confluent monolayer was observed in the culture dish around day 10.

Gene expression

The effect of co-culture on the transcription of both chondrocyte- and osteoblast-specific markers was examined over time. Type II collagen gene expression was only observed in co-culture and chondrocyte micromass control groups with no visible difference between these two groups. Aggrecan expression was seen in all three groups, while type X collagen expression was not seen in any of the groups during the experiment.

Collagen deposition

As shown in Fig. 4, during co-culture, osteoblasts produced a predominantly type I collagen matrix (Fig. 4A) and chondrocytes within the micromass continued to produce type II collagen (Fig. 4B). Type I collagen deposition was limited to the top of the micromass where osteoblasts were located, while type II collagen was seen primarily within the micromass during co-culture. Type I collagen was found in the monolayer surrounding the micromass (Fig. 4A) and in the osteoblast monolayer control. Minimal background staining for type II collagen (Fig. 4B) was observed in the monolayer surrounding the micromass.

Total GAG deposition

As shown in Fig. 5, chondrocyte micromass controls continued to produce GAG, with proteoglycan deposition peaking at day 7. In contrast, significantly lower ($p < 0.05$) GAG content was measured for the co-cultured group over the 3-week period. As expected, minimal GAG content was measured for osteoblast control group.

Deposition of GAG matrix was visualized via Alcian blue staining. Both whole mount and cross-sections of the co-culture and control micromasses were examined. As seen in Fig. 6A, the highest GAG staining intensity was observed in the day 7 chondrocyte control. With the exception of day 1, GAG staining intensity was visibly lower in the co-culture group compared to the control. These findings are consistent with the quantitative GAG results (Fig. 5). Alcian blue staining of the cross-sections of the co-culture samples revealed characteristic peri-cellular GAG deposition within the chondrocyte micromass, while little or no positive staining was observed on the top portion of the sample where the osteoblasts were located (Fig. 6B). GAG was not detected in the monolayer surrounding the micromass in co-culture.

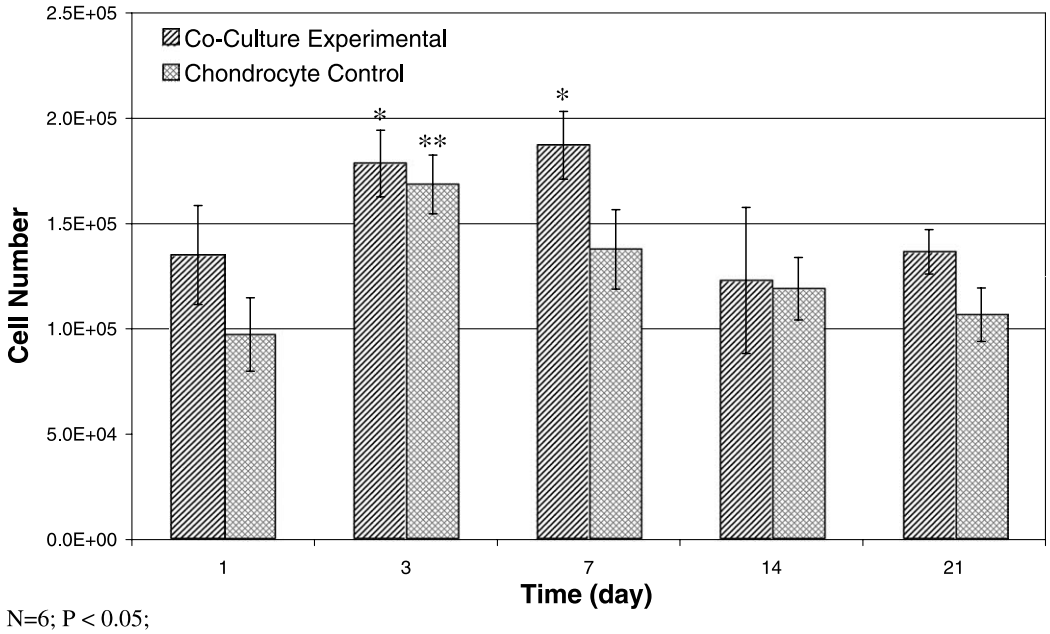

N=6; P < 0.05;
* Significantly different from all other groups.
** Significantly different from day 1, 14, and 21 controls.

Fig. 3. Effects of co-culture on cell growth, measured with total DNA content (7.7 pg DNA/cell). Cell number within the micromass remained relatively constant over time.

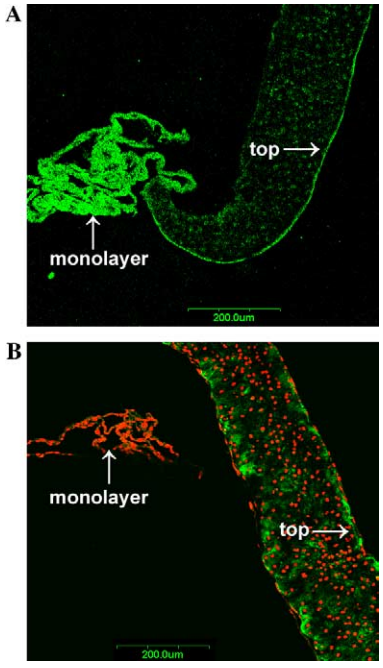

Fig. 4. Type I (A) and II (B) collagen distribution within the co-cultured micromass (day 11). Type I collagen was mainly deposited at the top surface and the surrounding monolayer, where cells had flattened. Type II collagen was distributed within the micromass and only minimal background staining was seen in the surrounding monolayer. Propidium iodide (red) nuclear stain was used to visualize cells. (For interpretation of the references to color in this figure legend, the reader is referred to the web version of this paper.)

Alkaline phosphatase activity and mineralization

As shown in Fig. 7, the average ALP activity in the co-cultured group was higher than chondrocyte control for the duration of the experiment. As expected, the chondrocyte micromass control showed minimal ALP activity. When β-GP was added to the media at day 7, while there was a measurable increase in ALP activity in the chondrocyte micromass control group, the level of ALP activity was significantly lower than the co-cultured group ($p < 0.05$). In the co-cultured group, there was an initial increase in ALP activity, reaching a maximum at day 11 and decreasing thereafter. A similar trend was observed for the osteoblast monolayer control.

The effects of co-culture on the formation of a mineralized matrix are presented in Fig. 8. The ALZ staining intensity for the osteoblast control became increasingly positive over time while background level staining was observed for micromass group. Since the micromass is of five to ten cell layers in thickness, the background staining intensity was considerably higher compared to the positive control (osteoblast monolayer). Moreover, similar staining intensity was observed for the co-cultured micromass (Fig. 8B) compared to the whole mount chondrocyte micromass control (Fig. 8A) which does not mineralize. The staining intensity of the both chondrocyte control and co-culture group remains relatively constant over time, whereas the osteoblast control stained increasingly positive for a mineralization matrix.

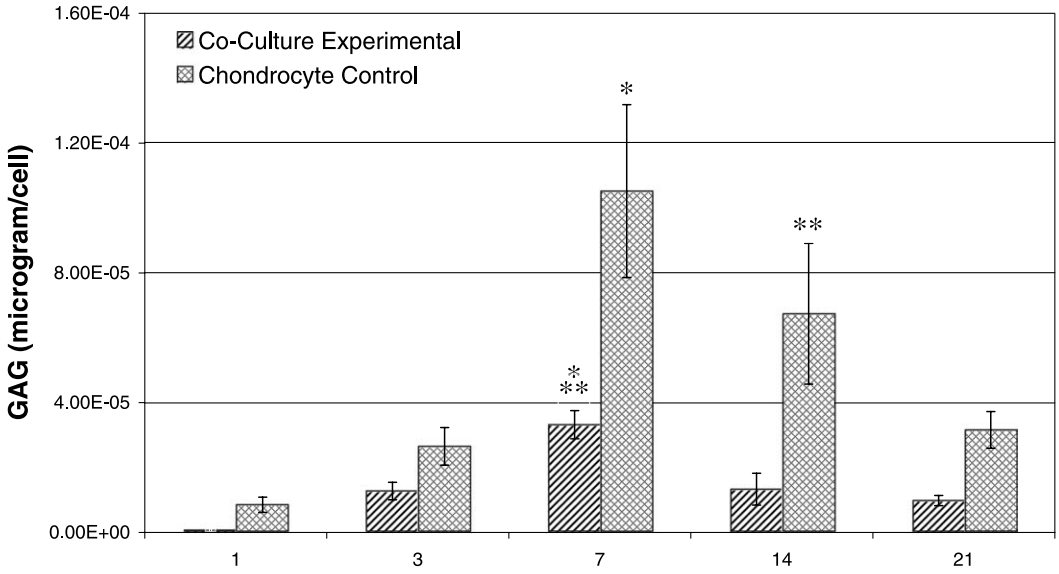

N=5; P<0.05;
* Significantly different from all other group.
** Significantly different from all groups except day 3 control and day 7 co-culture.
*** Significantly different from all groups except day 3 co-culture, day 3 and 21 controls.

Fig. 5. Total GAG content within the micromass normalized to total cell number. A maximum was found on day 7. Chondrocyte control had significantly greater GAG content compared to experimental group after 3 days. Osteoblast control showed minimal GAG deposition.

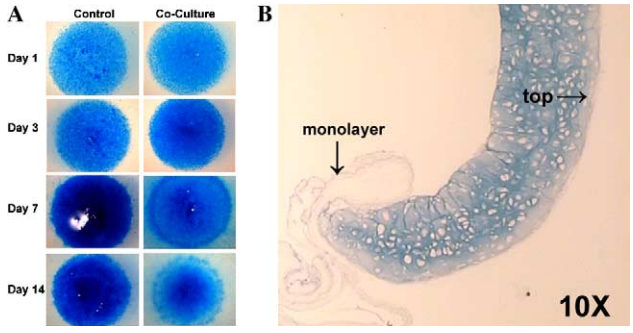

Fig. 6. Alcian blue staining for GAG deposition within the micromass. (A) Whole mount staining displayed an increase in intensity with time, which reached a maximum at day 7. (B) Cross-section of a co-cultured micromass at day 14. Notice the characteristic peri-cellular distribution of GAG within the micromass. Chondrocyte controls showed more intense staining compared to co-culture experimental groups after 3 days.

Discussion

The objective of this study was to develop a physiologically relevant co-culture model that can be used to evaluate interactions between osteoblasts and chondrocytes. We have described here a co-culture model which allows for direct cell-to-cell contact as well as paracrine signaling between osteoblasts and chondrocytes. This model was subsequently used to examine osteoblast and chondrocyte interaction, and it was found that cell–cell interactions had marked effects on matrix production and the expression of cell-specific markers.

The co-culture model presented here is based on the establishment of an osteoblastic monolayer over a high density chondrocyte micromass. The micromass culture system was chosen because it has been shown to preserve chondrocyte phenotype and induce the chondrogenic phenotype [34,35]. High density micromass culture is a simple and elegant model that permits the maintenance of chondrocyte morphology and differentiation in the absence of a three-dimensional scaffold. It was first used by Ahrens et al. [28] to examine the chondrogenic potential of limb-bud mesenchymal cells in vitro, and the chondrogenic potential of pluripotent cells has since been validated in vitro using the micromass system [33,34,36–38].

In this study, no significant effect on cell proliferation was observed due to co-culture. Although cells did not proliferate within the micromass, they migrated from the micromass and proliferated in monolayer after 7 days of culture. Co-culture of osteoblasts and chondrocytes resulted in selective maintenance and suppression of certain chondrocyte- and osteoblast-specific markers. In co-culture, chondrocytes within the micromass elaborated GAGs and type II collagen. Similarly, osteoblasts produced type I collagen and maintained ALP activity in co-culture. Nevertheless, both quantitative and qualitative GAG analyses revealed that co-culture significantly reduced the production of proteoglycans by chondrocytes in comparison to chondrocyte controls. Osteoblast mineralization was also suppressed in co-culture. There was limited mineralization in the co-cultured group, while the osteoblast control stained increasingly positive for calcium over time. Thus, co-culture with chondrocytes may have delayed osteoblast-mediated mineralization. As the ratio of osteoblasts to chondrocytes in the co-culture

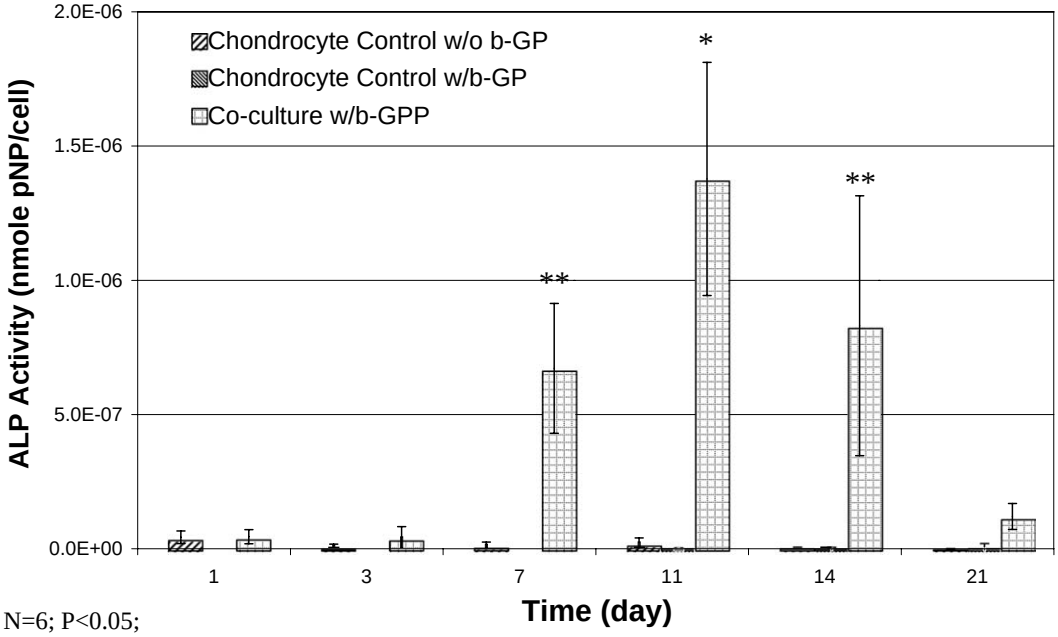

Fig. 7. Alkaline phosphatase activity normalized to total cell number. Active ALP was highest in the co-culture experimental group with β-GP. The experimental micromass group showed an initial increase that reached a maximum at day 11, and decreased thereafter. Osteoblast controls showed a similar trend.

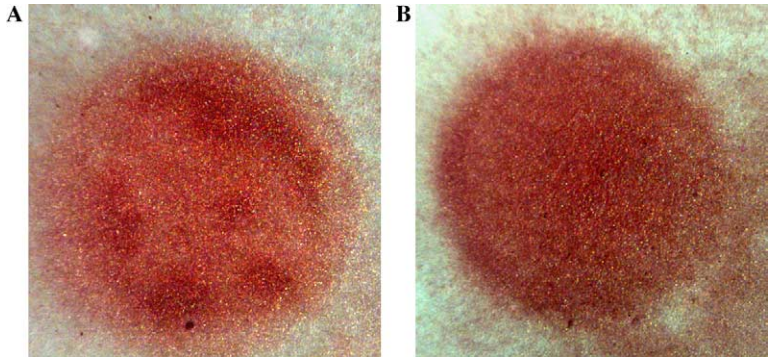

Fig. 8. Whole mount Alizarin red S staining. (A) Chondrocyte micromass control with β-GP. (B) Co-cultured experimental group with β-GP. No difference was seen between chondrocyte micromass and co-culture experimental groups. Stain intensity remained relatively the same through out the experiment for all micromass groups.

model was 1:4, we believe that the majority of the response in terms of GAG production can be attributed to chondrocytes, while ALP activity and mineralization can be attributed to osteoblasts. These findings collectively suggest that osteoblast–chondrocyte interactions regulate the metabolic activity, matrix production, and maintenance of specific cell phenotypes.

As type I and II collagen were both detected at the surface, it is possible that due to co-culture, chondrocytes and osteoblasts are forming an osteochondral-like interface at the surface interaction zone. The findings of this study suggest that during co-culture, rather than maintaining their individual phenotypes, osteoblasts and chondrocytes are instead responding to the presence of the other cell type. Osteoblast–chondrocyte co-culture may lead to the secretion of factors by either osteoblasts or chondrocytes which can in turn affect the response of neighboring cells that are responsible for the formation of the osteochondral interface. Still, it is not possible at this time to discern whether our findings are a direct result of cell–cell contact or of paracrine signaling between the adjacent osteoblast and chondrocyte populations.

While the primary focus of this study was to establish a co-culture model and examine the initial consequence of osteoblast and chondrocyte interactions, we also evaluated gene expression for type X collagen, which was not detected in any of the experimental groups. One limitation of the micromass system is that the 3-D culture of chondrocytes

cannot be maintained after 2 or 3 weeks of culture, largely due to cell migration out of the micromass and onto the coverslips. Therefore, micromass cultures in general do not exceed 3 weeks. Long-term co-culture models to test the expression of specific interfacial markers such as type X collagen will be explored in future studies. The co-culture model will also be utilized in future studies to study the effects of cell–cell interactions on the development of interface-specific markers.

Conclusions

Our results demonstrate a heterogeneous effect on both osteoblastic and chondrogenic phenotypes due to co-culture. The co-culture model permits physical interactions between osteoblasts and chondrocytes, while maintaining the chondrogenic phenotype within the micromass. It was found that co-culture had no effect on type I collagen production by osteoblasts, but interactions with chondrocytes may have delayed osteoblast-mediated mineralization. The effects of co-culture on chondrocytes were evident at the surface interaction zone, particularly in GAG and collagen deposition. Future studies will utilize this co-culturing system to investigate the relevance of osteoblast–chondrocyte interactions in the regeneration of the osteochondral interface.

Acknowledgments

The monoclonal antibody (II-II6B3) developed by T.F. Linsenmayer was obtained from the Developmental Studies Hybridoma Bank developed under the auspices of the NICHD and maintained by The University of Iowa, Department of Biological Sciences, Iowa City, IA 52242.

References

[1] Center for Disease Control Statistics, 2002.
[2] D.W. Jackson, M.J. Scheer, T.M. Simon, Cartilage substitutes: overview of basic science and treatment options, J. Am. Acad. Orthop. Surg. 9 (2001) 37–52.
[3] S.W. O'Driscoll, F.W. Keeley, R.B. Salter, The chondrogenic potential of free autogenous periosteal grafts for biological resurfacing of major full-thickness defects in joint surfaces under the influence of continuous passive motion. An experimental investigation in the rabbit, J. Bone Joint Surg. Am. 68 (1986) 1017–1035.
[4] H.A. Breinan, T. Minas, H.P. Hsu, S. Nehrer, S. Shortkroff, M. Spector, Autologous chondrocyte implantation in a canine model: change in composition of reparative tissue with time, J. Orthop. Res. 19 (2001) 482–492.
[5] E.B. Hunziker, Articular cartilage repair: are the intrinsic biological constraints undermining this process insuperable? Osteoarthritis Cartilage 7 (1999) 15–28.
[6] K. Masuda, R.L. Sah, M.J. Hejna, E.J. Thonar, A novel two-step method for the formation of tissue-engineered cartilage by mature bovine chondrocytes: the alginate-recovered-chondrocyte (ARC) method, J. Orthop. Res. 21 (2003) 139–148.
[7] S.H. Chia, B.L. Schumacher, T.J. Klein, E.J. Thonar, K. Masuda, R.L. Sah, D. Watson, Tissue-engineered human nasal septal cartilage using the alginate-recovered-chondrocyte method, Laryngoscope 114 (2004) 38–45.
[8] L.E. Freed, A.P. Hollander, I. Martin, J.R. Barry, R. Langer, G. Vunjak-Novakovic, Chondrogenesis in a cell-polymer-bioreactor system, Exp. Cell Res. 240 (1998) 58–65.
[9] M.D. Buschmann, Y.A. Gluzband, A.J. Grodzinsky, J.H. Kimura, E.B. Hunziker, Chondrocytes in agarose culture synthesize a mechanically functional extracellular matrix, J. Orthop. Res. 10 (1992) 745–758.
[10] R.L. Mauck, M.A. Soltz, C.C. Wang, D.D. Wong, P.H. Chao, W.B. Valhmu, C.T. Hung, G.A. Ateshian, Functional tissue engineering of articular cartilage through dynamic loading of chondrocyte-seeded agarose gels, J. Biomech. Eng. 122 (2000) 252–260.
[11] R.L. Mauck, S.L. Seyhan, G.A. Ateshian, C.T. Hung, Influence of seeding density and dynamic deformational loading on the developing structure/function relationships of chondrocyte-seeded agarose hydrogels, Ann. Biomed. Eng. 30 (2002) 1046–1056.
[12] R.L. Mauck, C.C. Wang, E.S. Oswald, G.A. Ateshian, C.T. Hung, The role of cell seeding density and nutrient supply for articular cartilage tissue engineering with deformational loading, Osteoarthritis Cartilage 11 (2003) 879–890.
[13] R. Tuli, W.J. Li, R.S. Tuan, Current state of cartilage tissue engineering, Arthritis Res. Ther. 5 (2003) 235–238.
[14] M. Ochi, Y. Uchio, M. Tobita, M. Kuriwaka, Current concepts in tissue engineering technique for repair of cartilage defect, Artif. Organs 25 (2001) 172–179.
[15] S.N. Redman, S.F. Oldfield, C.W. Archer, Current strategies for articular cartilage repair, Eur. Cell Mater. 9 (2005) 23–32.
[16] D. Schaefer, I. Martin, P. Shastri, R.F. Padera, R. Langer, L.E. Freed, G. Vunjak-Novakovic, In vitro generation of osteochondral composites, Biomaterials 21 (2000) 2599–2606.
[17] D. Schaefer, I. Martin, G. Jundt, J. Seidel, M. Heberer, A. Grodzinsky, I. Bergin, G. Vunjak-Novakovic, L.E. Freed, Tissue-engineered composites for the repair of large osteochondral defects, Arthritis Rheum. 46 (2002) 2524–2534.
[18] J.K. Sherwood, S.L. Riley, R. Palazzolo, S.C. Brown, D.C. Monkhouse, M. Coates, L.G. Griffith, L.K. Landeen, A. Ratcliffe, A three-dimensional osteochondral composite scaffold for articular cartilage repair, Biomaterials 23 (2002) 4739–4751.
[19] J. Gao, J.E. Dennis, L.A. Solchaga, V.M. Goldberg, A.I. Caplan, Repair of osteochondral defect with tissue-engineered two-phase composite material of injectable calcium phosphate and hyaluronan sponge, Tissue Eng. 8 (2002) 827–837.
[20] A. Alhadlaq, J.J. Mao, Tissue-engineered osteochondral constructs in the shape of an articular condyle, J. Bone Joint Surg. Am. 87 (2005) 936–944.
[21] R.M. Schek, J.M. Taboas, S.J. Segvich, S.J. Hollister, P.H. Krebsbach, Engineered osteochondral grafts using biphasic composite solid free-form fabricated scaffolds, Tissue Eng. 10 (2004) 1376–1385.
[22] R. Tuli, S. Nandi, W.J. Li, S. Tuli, X. Huang, P.A. Manner, P. Laquerriere, U. Noth, D.J. Hall, R.S. Tuan, Human mesenchymal progenitor cell-based tissue engineering of a single-unit osteochondral construct, Tissue Eng. 10 (2004) 1169–1179.
[23] H.H. Lu, J. Jiang, A. Tang, C.T. Hung, X.E. Guo, Development of controlled heterogeneity on a polymer-ceramic hydrogel scaffold for osteochondral repair, Bioceramics 17 (2005) 607–610.
[24] S. Lacombe-Gleize, M. Gregoire, S. Demignot, C. Hecquet, M. Adolphe, Implication of TGF beta 1 in co-culture of chondrocytes-osteoblasts, In Vitro Cell. Dev. Biol. Anim. 31 (1995) 649–652.
[25] K.F. der Mark, V.F. Gauss, H.F. der Mark, P. Muller, Relationship between cell shape and type of collagen synthesised as chondrocytes lose their cartilage phenotype in culture, Nature 267 (1977) 531–532.
[26] J.P. Spalazzi, K.L. Dionisio, J. Jiang, H.H. Lu, Osteoblast and chondrocyte interactions during coculture on scaffolds, IEEE Eng. Med. Biol. Mag. 22 (2003) 27–34.
[27] S.F. El Amin, M. Attawia, H.H. Lu, A.K. Shah, R. Chang, N.J. Hickok, R.S. Tuan, C.T. Laurencin, Integrin expression by human osteoblasts cultured on degradable polymeric materials applicable for tissue engineered bone, J. Orthop. Res. 20 (2002) 20–28.

[28] P.B. Ahrens, M. Solursh, R.S. Reiter, Stage-related capacity for limb chondrogenesis in cell culture, Dev. Biol. 60 (1977) 69–82.
[29] Y.J. Kim, R.L. Sah, J.Y. Doong, A.J. Grodzinsky, Fluorometric assay of DNA in cartilage explants using Hoechst 33258, Anal. Biochem. 174 (1988) 168–176.
[30] C.C. Teixeira, M. Hatori, P.S. Leboy, M. Pacifici, I.M. Shapiro, A rapid and ultrasensitive method for measurement of DNA, calcium and protein content, and alkaline phosphatase activity of chondrocyte cultures, Calcif. Tissue Int. 56 (1995) 252–256.
[31] J.D. Bancroft, M. Gamble, Theory and Practice of Histological Techniques, Churchill Livingstone, Edinburgh, 2002.
[32] H. Puchtler, S.N. Meloan, M.S. Terry, On the history and mechanism of alizarin and alizarin red S stains for calcium, J. Histochem. Cytochem. 17 (1969) 110–124.
[33] S.B. Nicoll, A. Wedrychowska, N.R. Smith, R.S. Bhatnagar, Modulation of proteoglycan and collagen profiles in human dermal fibroblasts by high density micromass culture and treatment with lactic acid suggests change to a chondrogenic phenotype, Connect. Tissue Res. 42 (2001) 59–69.
[34] A.E. Denker, S.B. Nicoll, R.S. Tuan, Formation of cartilage-like spheroids by micromass cultures of murine C3H10T1/2 cells upon treatment with transforming growth factor-beta 1, Differentiation 59 (1995) 25–34.
[35] A.L. Boskey, D. Stiner, I. Binderman, S.B. Doty, Effects of proteoglycan modification on mineral formation in a differentiating chick limb-bud mesenchymal cell culture system, J. Cell. Biochem. 64 (1997) 632–643.
[36] K. Daniels, R. Reiter, M. Solursh, Micromass cultures of limb and other mesenchyme, Methods Cell Biol. 51 (1996) 237–247.
[37] A.E. Denker, A.R. Haas, S.B. Nicoll, R.S. Tuan, Chondrogenic differentiation of murine C3H10T1/2 multipotential mesenchymal cells: I. Stimulation by bone morphogenetic protein-2 in high-density micromass cultures, Differentiation 64 (1999) 67–76.
[38] A. Muraglia, A. Corsi, M. Riminucci, M. Mastrogiacomo, R. Cancedda, P. Bianco, R. Quarto, Formation of a chondro-osseous rudiment in micromass cultures of human bone-marrow stromal cells, J. Cell Sci. 116 (2003) 2949–2955.